Journal of Science and Technology in Civil Engineering, HUCE, 2024, 18 (4): 12–29

ANALYSIS OF THE EFFECT OF CONSTRUCTION TECHNOLOGY FACTORS ON CONTROLLING THERMAL CRACKING IN MASS CONCRETE

Le Van Minh[a], Nguyen Anh Duc[a], Ho Ngoc Khoa[a], Le Hong Ha[a], Luu Van Thuc[a,*]

[a]*Faculty of Building and Industrial Construction, Hanoi University of Civil Engineering, 55 Giai Phong road, Hai Ba Trung district, Hanoi, Vietnam*

Article history:
Received 02/8/2024, Revised 25/10/2024, Accepted 09/12/2024

Abstract

A comprehensive numerical study was conducted in this study to evaluate the effects of construction technology factors including curing temperature, initial temperature of fresh concrete mixture, type of formwork, type of cement, and cement content on controlling thermal cracking in mass concrete. The probability of cracking will also be included in the analysis to align with the trend of thermal cracking control planning in some countries today. Stress-temperature field analysis will be performed using the finite element heat flow analysis tool of Midas/Civil software. The reliability and accuracy of the proposed method are verified by comparing the analysis results with a experimental result of a mass concrete sample with dimensions of 2.5 × 2.5 × 2.5 m. Based on the validated numerical model, a parametric study was conducted on a typical mass concrete block with dimensions 5.0 × 5.0 × 5.0 m to investigate the impact of construction technology parameters on temperature development in mass concrete. The obtained results demonstrate that construction technology factors significantly affect thermal cracking in mass concrete. An effective construction solution will contribute significantly to the overall plan for controlling thermal cracking in mass concrete.

Keywords: mass concrete; thermal cracking index; heat of hydration; construction technology; thermal stress.

https://doi.org/10.31814/stce.huce2024-18(4)-02

1. Introduction

Constructing mass concrete often encounters challenges and requirements in controlling temperature rise, as the cement hydration process can lead to thermal cracking. Excessive heat generation will result in temperature differences between the surface and the interior of the mass concrete, causing cracks when thermal tensile stress exceeds allowable tensile stress [1–6]. Thermal cracks can compromise the integrity, stability, and lead to harmful effects on the structure [7]. In the USA, the ACI 207 committee has issued a set of standards for mass concrete, consisting of five component standards [8–12]. In 2008, the Japan Concrete Institute (JCI) revised and issued technical guidelines for controlling thermal cracking in mass concrete [1]. In the UK, regulations for mass concrete construction can be found in Part 1 of the BS 8110 standard [13]. In Russia, some regulations on mass concrete can be found in standard [14]. In Vietnam, requirements for mass concrete construction are specified in standard TCVN 9341:2012 [15]. Most of the current global standards and technical guidelines for controlling thermal cracking in mass concrete aim at three main goals: (i) controlling the core temperature of the concrete block not to exceed 70 °C during the early stages of cement hydration to avoid the formation of delayed ettringite (DEF) [16], thus preventing late-stage cracks due to ettringite expansion; (ii) controlling the temperature difference between the surface and the interior of the block

*Corresponding author. *E-mail address:* thuclv@huce.edu.vn (Thuc, L. V.)

not to exceed 20 °C to 25 °C. The heat generated from the cement hydration with the slow heat dissipation rate within the concrete mass is the main reason of the temperature increase within the mass concrete. Concrete in the core with high heat tends to expand while the exterior surface, exposed to the environment, tends to contract and restricts the expansion of the interior concrete. This causes tensile stress on the surface concrete, leading to thermal cracking when thermal tensile stress exceeds allowable tensile stress [2, 16]; and recently in Japan; (iii) the evaluation of crack formation in mass concrete is conducted using the thermal cracking index, which predicts the tendency for cracking [1]. Therefore, technologies to control thermal cracking in mass concrete aim to address the three main phenomena mentioned above.

While existing standards and guidelines provide valuable frameworks for controlling thermal cracking, the increasing scale and complexity of modern construction projects demand further investigation into the influence of construction technology and other uncontrolled factors. Given the changes in the context of modern mass concrete construction, with more super-tall buildings and new modern construction technologies, researching the impact of construction technology on controlling thermal cracking in mass concrete is necessary. In Vietnam, reinforced concrete structures are significantly increasing. Specifically, (i) the foundation mat of the Lotte Center Hanoi has a volume of up to 18600 m^3, dimensions of 44.1 × 92.7 × 5.7 m; (ii) the foundation of the Bitexco Financial Tower in Ho Chi Minh City is up to 4.0 m thick; (iii) the foundation mat of the Keangnam Hanoi Landmark Tower has a volume of nearly 24870 m^3, a surface area of 6217 m^2, and is also 4.0 m thick; and most recently, the Landmark 81 Tower in Ho Chi Minh City has a foundation mat surface area of 3000 m^2, a thickness of 8.4 m, and a concrete volume of nearly 17000 m^3. Additionally, conclusions mentioned in current standards are drawn from experiments where construction technology factors are rarely considered. Thus, surveys on the impact of construction technology factors on thermal cracking are needed for more accurate conclusions. Furthermore, during construction, uncontrollable random factors during the design stage such as weather, contractor skill level, and type of aggregates used can also lead to cracking risks for the concrete block. Therefore, it is necessary to include the probability of cracking in the analysis [1, 17].

In this study, a comprehensive investigation into the effects of construction technology on controlling thermal cracking in mass concrete will be conducted. Stress-temperature field analysis will be performed using the finite element heat flow analysis tool of Midas/Civil software. Important construction technology factors affecting the control of thermal cracking in mass concrete will be investigated, including curing temperature, initial temperature of fresh concrete mixture, type of formwork, type of cement, and cement content on the thermal cracking index. The probability of cracking will also be included in the analysis to align with the trend of thermal cracking control planning in some countries today. The reliability and accuracy of the proposed method are verified by comparing the analysis results with experimental results. The obtained results demonstrate that construction technology factors significantly affect thermal cracking in mass concrete. An effective construction solution will contribute significantly to the overall plan for controlling thermal cracking in mass concrete. Throughout the study, bold letters denote matrices or vectors in the formulations.

2. Mathematical foundations of the heat of hydration analysis of mass concrete

During the initial stages of concrete, heat will be generated through the chemical reactions between cementitious materials and water. Heat of hydration analysis can be conducted through 2 main processes: (i) heat transfer analysis, and (ii) thermal stress analysis. Heat transfer analysis determines how nodal temperatures change over time due to factors like heat sources, convection, and conduction involved in the cement hydration process. Thermal stress analysis then calculates the resulting stress

in mass concrete at each stage based on these temperature changes over time. These calculations also incorporate material property changes dependent on time and temperature, time-dependent shrinkage, and creep influenced by both time and stress.

2.1. The heat conduction process in concrete

Numerical modeling of the transient temperature problem, considering the heat release during cement hydration, is based on solving the well-known thermal conductivity equation [18–21], as described by the below equation:

$$\rho C \frac{\partial T}{\partial t} = \lambda \nabla^2 T + q_V \tag{1}$$

where T represents the temperature at a specific element at time t (°C); λ denotes the thermal conductivity coefficient of the material being considered (W/m °C); q_V describes the amount of heat generated within a unit volume of the material (W/m^3); C denotes the concrete's specific heat capacity, which is the amount of heat required to raise the temperature of one kilogram of concrete by one degree Celsius (J/kg °C); ρ is the density of concrete (kg/m^3); and t is the time.

Eq. (1) can be presented in matrix form as below:

$$\mathbf{C}\dot{\mathbf{T}} + \overline{\mathbf{K}}\mathbf{T} = \mathbf{Q} \tag{2}$$

where $\mathbf{C}$ is the specific heat capacity matrix; $\overline{\mathbf{K}}$ presents the thermal conductivity matrix including conduction and convection; $\mathbf{Q}$ denotes the total heat flux vector for internal hydration and thermal convection; $\mathbf{T}$ is the nodal temperature vector; and $\dot{\mathbf{T}}$ denotes the time derivative of the nodal temperature vectors.

The thermal conductivity coefficient in concrete generally decreases with rising temperature, especially near ambient temperature [21, 22]. Boundary conditions for Eqs. (1) and (2) are described in the following equations.

At a constant temperature boundary, which is the temperature boundary condition of the foundation soil

$$-k \frac{\partial T}{\partial n} = 0 \tag{3}$$

where k is the direction cosine of the heat transfer surface under consideration corresponding to the three spatial directions x, y, z and T represents the temperature at the boundary (°C).

At the heat transfer boundary, which is the interface between the concrete layers

$$-k \frac{\partial T}{\partial n} = q_V \tag{4}$$

in which q_V is the heat generated per unit volume at time t (kcal/m^3).

At the convection boundary, referring to the concrete surface in contact with either the formwork or the environment

$$-k \frac{\partial T}{\partial n} = h_c (T - T_\infty) \tag{5}$$

here h_c is the convection coefficient (kcal/m^2.h.°C), T denotes the temperature at the convection surface (°C), T_∞ is the ambient temperature (°C), and n is the direction cosine of the heat transfer surface under consideration.

2.2. Heat source

According to references [1, 23], the amount of heat generated per unit volume of concrete and the corresponding concrete temperature at various times during curing are established using Eqs. (6) and (7), as follows:

$$q_V = \frac{1}{24}\rho C K e^{\frac{-\alpha t}{24}} \tag{6}$$

$$T(t) = K(1 - e^{-\alpha t}) \tag{7}$$

where q_V is the heat generated per unit volume (kcal/m^3); ρ presents the density of concrete (kg/m^3); C is the specific heat capacity of concrete (kcal/kg.°C); t is time (days); α denotes the coefficient that indicates the extent of hydration, which ranges from 0 to 1; K describes the highest temperature of concrete under adiabatic conditions (°C); $T(t)$ denotes the temperature of concrete material at age t (days) during heat curing (°C).

The degree of hydration in mass concrete α is influenced by various factors, including the cement content, the initial temperature of the concrete mixture, and the age of the concrete.

2.3. The relationship between stress and temperature fields

According to references [1, 24], an increase in the temperature differential ΔT leads to a corresponding increase in thermal stress within the concrete mass. This connection between thermal stress and temperature differential is mathematically expressed by Eq. (8):

$$\boldsymbol{\sigma} = \mathbf{E}\boldsymbol{\beta}\mathbf{R}\Delta\mathbf{T} \tag{8}$$

where $\boldsymbol{\sigma}$ is the stress vector at the surveyed point (Kgf/m^2); $\mathbf{R}$ denotes the strain resistance matrix of concrete, which describes how concrete resists deformation under various stresses and conditions and ranges from 0 to 1; $\mathbf{E}$ presents the concrete modulus of elasticity (Kgf/m^2); $\Delta\mathbf{T}$ is the temperature gradient vector; and $\boldsymbol{\beta}$ is the thermal expansion coefficient of concrete.

The thermal crack index I_{cr} of a concrete structure is defined as the ratio of tensile splitting strength to the tensile stress induced by temperature changes throughout the thermal process. This concept of thermal crack index I_{cr} is proposed in the guidelines of the Japan Concrete Institute [1] and the Korea Concrete Institute [25]. Formula (9) provides the calculation method for I_{cr}, as follows:

$$I_{cr} = \frac{f_t(t)}{\sigma_t(t)} \tag{9}$$

$$f_t(t) = C_1\left[t(a + bt)^{-1} f'_c(28)\right]^{C_2} \tag{10}$$

where $f_t(t)$ is the design value of splitting tensile strength of concrete at time t (Kgf/m^2), determined by formula (10); $\sigma_t(t)$ defines the tensile stress in the concrete structure at a given time t (Kgf/m^2); C_1, C_2 are constants that vary depending on the type of concrete; $f'_c(t)$ denotes the compressive strength of concrete at age t (Kgf/m^2). In this study, the development of compressive strength of concrete over time is determined according to ACI standards; t denotes the age of considering time (days); a, b are factors which influence how the compressive strength of concrete develops over time, depending on the type of concrete used. In this study, a, b are referred to Table 1; and $f'_c(28)$ shows the concrete's compressive strength after 28 days.

Table 1. Material and thermal properties

Property	Unit	Concrete	Subsoil
Specific heat	kcal/kg°C	0.25	0.2
Density	kgf/m^3	2500	1800
Heat conduction coefficient	kcal/m.h.°C	2.3	1.7
Ambient temperature	°C	20	-
Compressive strength gain coefficients	ACI	$a = 13.9$, $b = 0.86$	-
Modulus of elasticity	kG/cm^2	2.7734×10^5	1.0×10^4
Thermal expansion coefficient		1.0×10^{-5}	1.0×10^{-5}
Poisson's ratio		0.18	0.2

2.4. The temperature parameters for finite element simulation

a. Specific heat capacity

According to the Japan Concrete Association [1], concrete's specific heat capacity typically ranges from 0.27 to 0.31 kcal/kg°C, whereas ACI 207.2R-07 [11] specifies a range of 0.22 to 0.24 kcal/kg°C. This paper adopts a specific heat capacity value of 0.25 kcal/kg°C, as in Table 1.

b. Thermal convection

The cumulative impact of natural convection is mathematically expressed by Newton's cooling law, as formulated in Eq. (11):

$$Q = h_c A \left(T_S - T_\infty\right) \tag{11}$$

where Q is the heat flux (kcal/h); h_c is the convection coefficient (kcal/m^2.h.°C); A denotes the surface area (m^2); T_s presents the temperature at the surface of the block (°C); and T_∞ is the ambient temperature (°C). It needs to be noted herein that the convection coefficient h_c depends on various factors including the type of flow, physical properties of the flow, average temperature of the surface in contact with convection, position, geometric structure, contact area with the flow, and other relevant parameters. Analyzing convection becomes particularly critical in the context of large concrete structures, where understanding temperature transfer between the concrete surface and the surrounding air is essential.

2.5. Probability of thermal cracking $P\left(I_{cr}\right)$

The quality of concrete structures is heavily influenced by cracks, making the prevention or control of cracks due to temperature crucial. The goal of a thermal crack control plan is to keep crack widths below permissible limits. In the analysis of concrete masses, determining whether a structure will develop cracks depends on whether the tensile strength of concrete exceeds the thermal tensile stress that arises within the concrete mass. However, a significant concern arises from the potential differences between the mechanical and thermal properties of concrete observed during design stage and those encountered in actual construction [1]. The Japan Concrete Institute has established a correlation between crack index I_{cr} and the probability of thermal cracks $P(I_{cr})$. This correlation is derived by comparing thermal crack indices obtained from three-dimensional finite element analyses of actual structures with observed data on whether thermal cracks have occurred. Formula (12) provides the method for determining the thermal crack probability of concrete structures, and

$$P\left(I_{cr}\right) = 1 - \exp\left[-\left(\frac{I_{cr}}{0.92}\right)^{-4.92}\right] \tag{12}$$

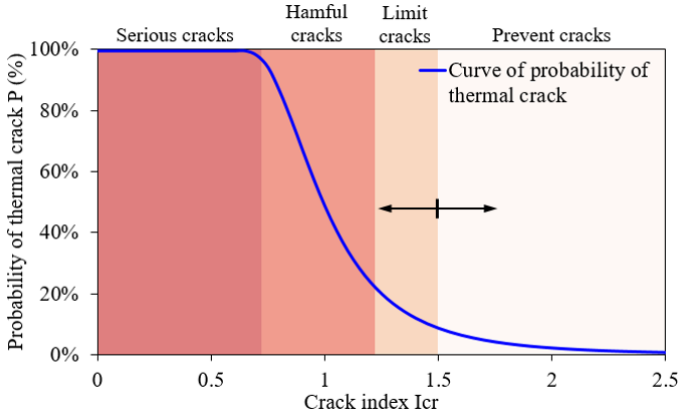

Figure 1. Correlation between crack index and thermal crack probability

In concrete engineering, a thermal crack is considered unlikely to appear when the crack index I_{cr} is below a certain threshold. This threshold indicates a low probability of thermal cracking occurring under typical conditions. According to the Japan Concrete Institute (JCI), for concrete structures, a crack index $I_{cr} \geq 1.85$ corresponds to a thermal crack probability $\leq 5\%$ at which a thermal crack is considered not to occur. If the crack probability exceeds 5%, the component is at a high risk of cracking. According to the technical standards of South Korea [25]: (i) to prevent thermal cracks, the crack index $I_{cr} \geq 1.5$; (ii) to limit the width of thermal cracks, $1.5 > I_{cr} \geq 1.2$; and (iii) to restrict harmful cracks $1.2 > I_{cr} \geq 0.7$. In this study, a crack index value of $I_{cr} = 1.5$ is chosen as the threshold to determine whether the concrete structure has cracks or not. During analysis, if the crack index of the concrete mass is $I_{cr} \geq 1.5$, it is concluded that the concrete mass does not have cracks, and vice versa, as illustrated in Fig. 1. Based on this, charts or formulas can be referenced to determine the corresponding crack index value. Measures taken to control thermal cracks must ensure that the crack index remains above the chosen threshold.

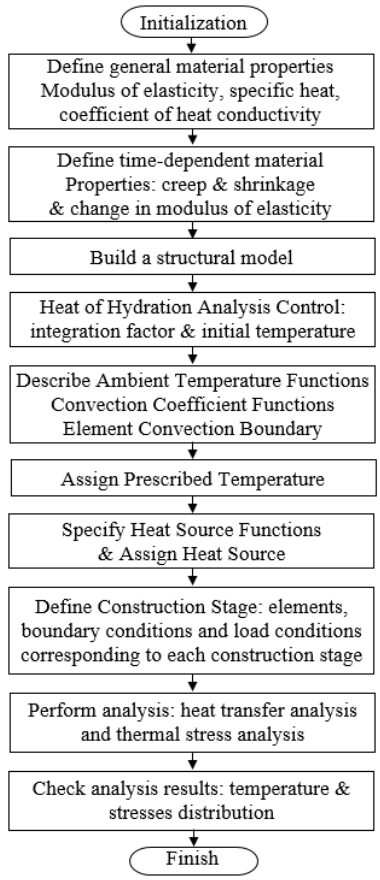

Figure 2. The process of analyzing the temperature-stress field in mass concrete

2.6. Process of analyzing the temperature-stress field in mass concrete using FEM

The temperature - stress field in mass concrete in this study is analyzed by using the FEM. In this study, MIDAS Civil software will be used for analyzing and investigating the numerical model. The process consists of 9 steps as illustrated in Fig. 2.

3. Verification

A large concrete sample with dimensions of 2.5 × 2.5 × 2.5 m will be tested, and the results obtained from numerical simulations will be compared with the experimental results. Concrete that have the strength grade of B30 and the slump of 16 ± 2 cm are used for this experiment. The mix proportions of the upper and lower layers of mass concrete are described in Table 2. The formwork system is made of steel formwork, which is braced with wooden battens that are combined with steel braces and diagonal supports. The outside of the formwork system is wrapped with insulation material to keep the heat within the concrete mass. During the construction phase, concrete material is placed continuously using a boom pump and thoroughly compacted, as illustrated in Figs. 3(c) and (d). After pouring the concrete and finishing the work of the concrete surface, a nylon layer and a insulation material layer are applied to mass concrete to prevent heat from escaping that concrete mass. Dry-cured is adopted. The temperature of the concrete mass on the curing surface is monitored to control the temperature difference between the center part and the surface part. The experimental equipment includes temperature sensors in the concrete mass and ground temperature sensors, a datalogger for data reading, curing temperature readers, formwork temperature readers, and an environmental temperature and humidity measurement unit. The temperature measurement positions within the concrete mass are shown in Fig. 3(a). There are three temperature measurement piles located at the center, edge, and corner of concrete mass. Each pile has six temperature measurement positions, as shown in Fig. 3(b), with two temperature sensors at each position. Placing two temperature sensors in one position ensures accurate temperature control, ensuring that even in unfavorable situations where a sensor fails, the results are still fully recorded. Thus, the concrete mass will have 36 temperature sensors at 18 positions. Temperature data for the curing layer's core, the formwork surface, and the ground are also collected. When the concrete mass temperature approaches the ambient temperature, the curing layer is removed. Note that the ambient temperature and humidity measurement process is continuously recorded, while in the first stage after pouring the concrete, when the temperature rises, the concrete temperature is measured every hour. After that, temperature is measured every 3 hours until the concrete temperature gradually stabilizes to ambient at 216 hours [26]. The stress-temperature field analysis is performed using the finite element heat analysis tool of Midas/Civil software [27]. The overall model includes 10000 solid elements and 11781 nodes, in which concrete mass model consisting of 1000 solid elements and 1210 nodes, and ground model consisting of 9000 solid elements and 10571 nodes, as shown in Fig. 3(e).

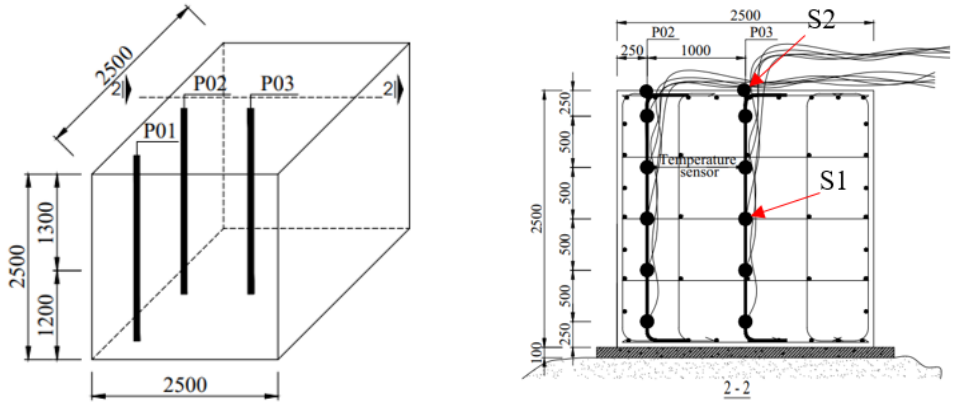

(a) Temperature sensor placement

(b) Details of the temperature probe

(c) Concrete pouring work

(d) On-site concrete block

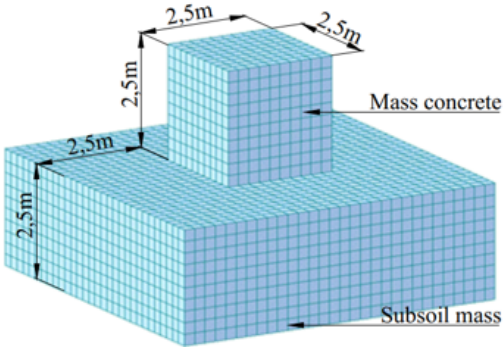

(e) Numerical simulation of the concrete

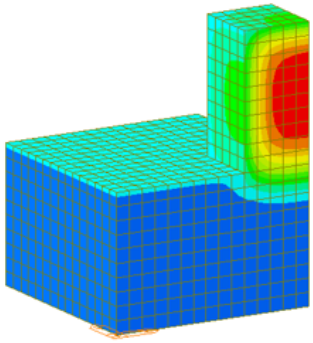

(f) Temperature field in the simulation

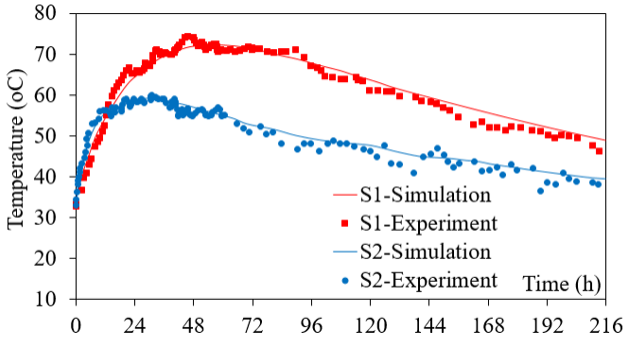

(g) Comparison of temperature development between simulation and experiment

Figure 3. Model and temperature regime of the mass concrete in the experiment

Table 2. Experimental concrete mix proportions

	Cement (kg/m^3)	Fly ash (kg/m^3)	Additive (kg/m^3)	Sand (kg/m^3)	Gravel (kg/m^3)	Water (kg/m^3)
Top layer (0.5 m)	385.0	-	3.80	858.5	1015.0	131.5
Bottom layer (2.0 m)	308.0	77.0	3.80	858.4	1015.2	131.6

The temperature field distribution of the concrete block is shown in Fig. 3(f), while the comparison of temperature results between simulation and experimental data shows that the measured

temperature development curve from the experimental concrete block and the numerical simulation are relatively close, as illustrated in Fig. 3(g). The similarity in temperature development and the maximum temperature values at the three investigated axes - center, edge, and corner demonstrates the reliability and accuracy of the numerical simulation process and method. The maximum temperature at the central axis predicted by the numerical model is $T_{\max}$ = 72.3 °C, compared to the experimental result of $T_{\max}$ = 74.4 °C, a difference of approximately 2.8%. The maximum temperature at the edge axis predicted by the numerical model is $T_{\max}$ = 59.1 °C, compared to the experimental result of $T_{\max}$ = 60.1 °C, a difference of about 1.7%. The similarity in the temperature development pattern and the maximum temperature values at the surveyed points demonstrates the reliability and consistency between simulation and experimentation. This result proves the reliability of the numerical simulation process using the Midas/Civil tool. Therefore, the extended simulation results presented in this paper are valuable and can accurately reflect the real behavior of the stress-temperature field in the concrete block.

4. Case study

The evaluation of the impact of construction technology factors on the effectiveness of controlling thermal cracking in mass concrete is based on three main criteria: (i) maximum temperature $T_{\max}$, surveyed at the center of the mass, (ii) temperature difference between the center and the surface of the mass ΔT, and (iii) thermal cracking index I_{cr}, surveyed at the edge where the tensile stress is highest. The criteria for controlling thermal cracking will be chosen based on the specific conditions of each project and the requirements of the investor. In this study, all three criteria will be used to provide a comprehensive view of the thermal cracking control criteria. When considering the probability of cracking, if the cracking index reaches $I_{cr} \leq 1.5$, the concrete structure will be considered to have begun cracking. Five key construction technology factors will be surveyed to assess the extent to which construction technology affects the effectiveness of controlling thermal cracking in mass concrete: (1) concrete curing temperature; (2) initial temperature of the fresh concrete mixture; (3) type of formwork; (4) type of cement; and 5) cement content used.

4.1. Numerical simulation model

The subject of the survey on the impact of construction technology is a typical large footing structure, including a soil mass with dimensions of 15.0 × 15.0 × 5.0 m and a concrete footing mass with dimensions of 5.0 × 5.0 × 5.0 m, as illustrated in Fig. 4(a). The concrete material and heat of hydration analysis data are used as shown in Table 2. The concrete mix design for the large footing of the Lotte Center building will be used in the study, with M400 or B35, as detailed in Table 3. The overall model includes 10000 solid elements and 11781 nodes, with the concrete mass model consisting of 1000 solid elements and 1210 nodes and the underlying soil mass model consisting of 9000 solid elements and 10571 nodes. Thermal boundary conditions of mass concrete are described in Fig. 4(b), meanwhile, the temperature distribution and cracking index in the mass concrete are illustrated in Figs. 4(c) and (d). It should be noted herein that the model is fully simulated and is shown with a 1/4 block for visualization purposes, and the subsoil is restrained by fixed connections. According to [1], modeling reinforcement in mass concrete is unnecessary because the obstruction caused by the reinforcement is generally insignificant, and thus, its impact on thermal stress is minimal. Many studies on thermal problems in mass concrete do not consider the simulation of reinforcement in the thermal analysis of mass concrete. In this study, reinforcement will be omitted in the model.

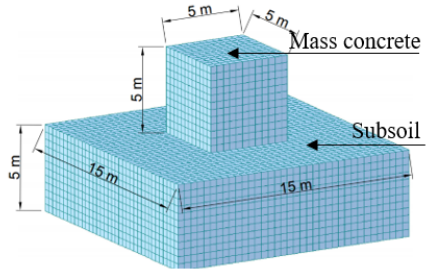

(a) Configuration of the mass concrete

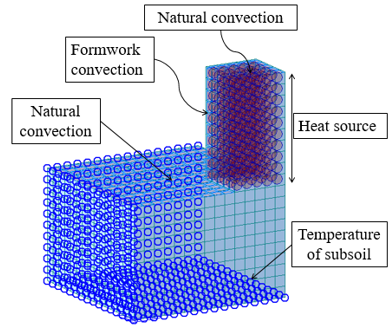

(b) Thermal boundary conditions

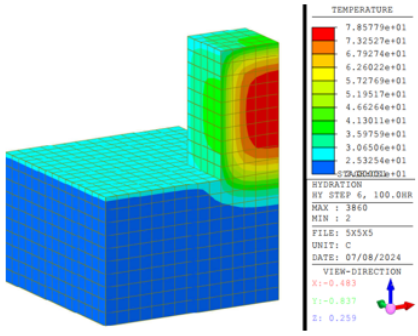

(c) Temperature distribution (1/4 block)

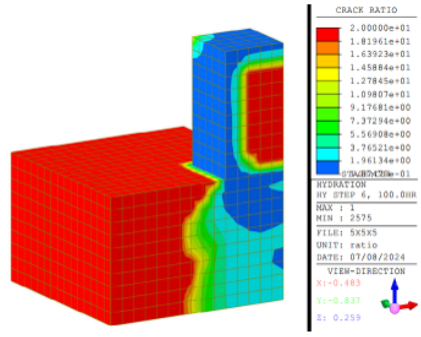

(d) Crack index distribution(1/4 block)

Figure 4. Model and temperature regime of the mass concrete

Table 3. Typical concrete mix composition

Sand (kg)	Gravel (kg)	Water (l)	Binder (kg/m^3)	Cement (%)	Fly ash (%)	Admixture (%Binder)
880	951	160	385	75	25	1.35

4.2. Numerical results and discussions

a. Effects of the curing temperature

To assess the impact of curing temperature on the development of the temperature field and thermal cracking index, four analysis models with input data as shown in Table 1 and Fig. 4, are subjected to varying curing temperature conditions around the block T_{cu} = 10 °C, 20 °C, 30 °C, and 40 °C. It is also important to note that when the curing temperature is adjusted, the ground temperature and the initial temperature of the concrete mixture will be maintained at 20°C, while other parameters will be kept at standard values.

The analysis results show that with the solution to control thermal cracking in large concrete blocks as mentioned above, as the curing temperature T_{curing} increases, the surface temperature of the block also increases. This minimizes the temperature gradient between the core and the surface of the concrete block. When the curing temperature T_{curing} increases from 10 °C to 40 °C, although the maximum temperature at the core $T_{\max}$ remains almost unchanged, the temperature difference ΔT decreases significantly from 45.9 °C to 22.4 °C, a reduction of more than 23.0 °C, as illustrated in Fig. 5(a) and Table 4. This is beneficial for a thermal cracking control plan, meaning that the

foundation block reduces the risk of thermal cracking. Considering the thermal cracking index I_{cr}, it can be seen that I_{cr} increases as the curing temperature increases. At 100 hours after pouring, the concrete block cured at T_{curing} = 40 °C has an I_{cr} = 0.92, while the block cured at T_{curing} = 30 °C has an I_{cr} = 0.80, and the block cured at T_{curing} = 10 °C has an I_{cr} = 0.60, as shown in Fig. 5(b) and Table 4. Clearly, with this thermal cracking control plan, the temperature difference between the core and the surface of the concrete block decreases as the curing temperature increases. This reduction in temperature difference reduces the tendency for the outer surface of the block to contract, thereby limiting tensile stress due to temperature.

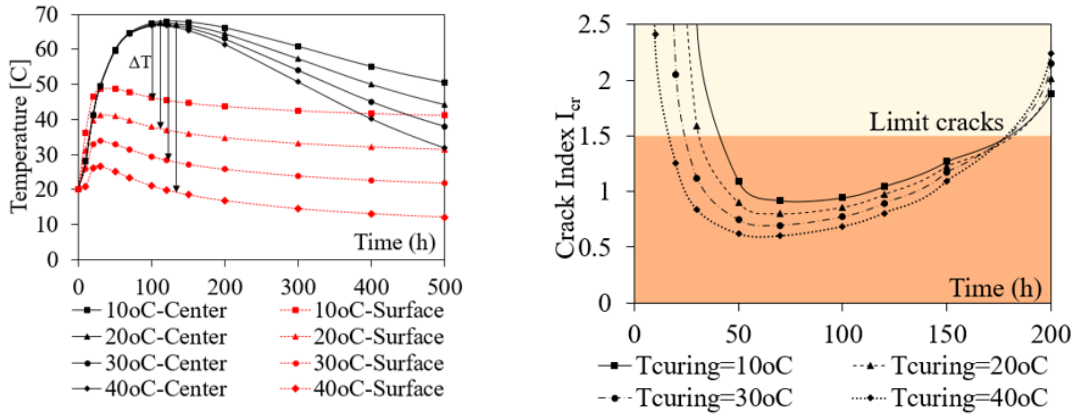

(a) The temperature gradient between the center and the surface

(b) Crack index

Figure 5. Effects of the curing temperature on the temperature regime of mass concrete

Table 4. Effect of curing temperature on the temperature regime in the mass concrete

No	Curing temperature	Temperature regime in the mass concrete			
		$T_{\max}$ (°C)	ΔT (°C)	I_{cr} (min)	Time (h)
1	10 °C	66.8	45.9	0.60	100
2	20 °C	67.2	38.7	0.69	120
3	30 °C	67.6	30.6	0.81	120
4	40 °C	67.9	22.4	0.92	120

b. Effects of the fresh concrete temperature

To evaluate the effect of the initial temperature of the fresh concrete mix on the thermal regime in mass concrete, the study analyzes four models, using input materials as shown in Table 1, analysis models as depicted in Fig. 4, and varying the temperature of the concrete mix T_{mix} = 10 °C, 20 °C, 30 °C, 40 °C. It should also be noted here that when the initial temperature is changed, the ground temperature will be fixed at 20 °C, the ambient temperature will be fixed at 30 °C, and other parameters will be fixed at common values.

The temperature development curves at the center and the surface of the mass concrete according to the initial temperature changes of the concrete mix are shown in Fig. 6(a), while the comparison chart of the corresponding cracking index is illustrated in Fig. 6(b). The analysis results show that the higher the mix temperature T_{mix} during pouring, the higher the maximum temperature at the center

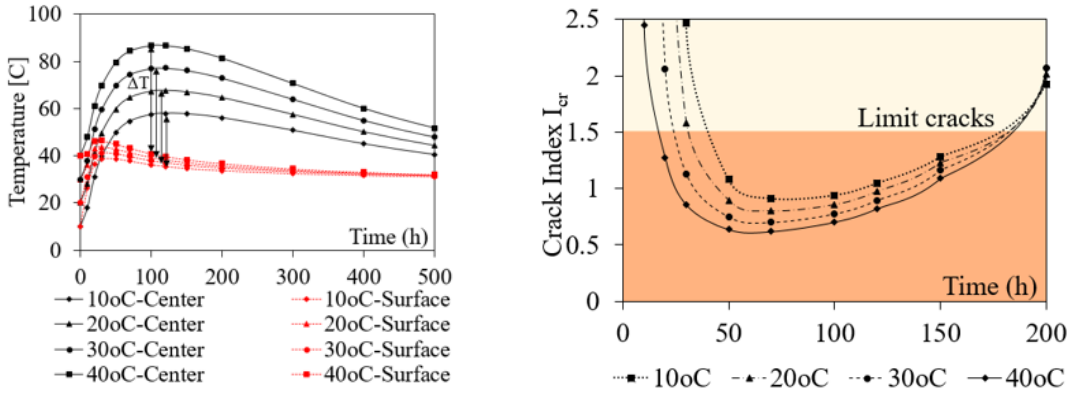

(a) The temperature gradient between the center and the surface

(b) Crack index

Figure 6. Effects of the fresh concrete temperature on the temperature regime of mass concrete

Table 5. Effects of fresh concrete temperature on the temperature regime in the mass concrete

No	Fresh concrete temperature	Temperature regime in the mass concrete			
		$T_{\max}$ (°C)	ΔT (°C)	I_{cr} (min)	Time (h)
1	10 °C	57.9	22.4	0.91	120
2	20 °C	67.5	30.6	0.80	120
3	30 °C	77.1	38.8	0.71	120
4	40 °C	86.8	46.9	0.61	100

$T_{\max}$ of the mass concrete. When the initial temperature of the concrete mix is T_{mix} = 10 °C, the maximum temperature at the center $T_{\max}$ = 57.9 °C, but when the initial temperature of the concrete mix increases to T_{mix} = 40 °C, the maximum temperature at the center also increases to $T_{\max}$ = 86.8 °C at 120 hours after pouring the concrete. Similarly, the temperature difference ΔT also tends to increase when the initial temperature of the concrete mix rises. For a concrete mix with an initial temperature T_{mix} = 10 °C, the temperature difference between the center and the surface of the mass concrete is ΔT = 22.4 °C, while for concrete mixes with initial temperatures of T_{mix} = 20 °C, 30 °C và 40 °C, the temperature differences are ΔT = 30.6 °C, 38.8 °C và 46.9 °C, respectively, as shown in Table 5. Considering the thermal cracking index, the mass concrete mix with an initial temperature T_{mix} = 10 °C has the highest cracking index I_{cr} = 0.91, indicating the lowest risk of cracking. In contrast, the concrete mix with an initial temperature T_{mix} = 20 °C has a cracking index I_{cr} = 0.80, and when the initial temperature of the concrete mix rises to T_{mix} = 40 °C, the concrete will have the lowest cracking index I_{cr} = 0.61, as shown in Table 5. It can be seen that with the analyzed conditions, reducing the initial temperature of the fresh concrete mix by 1 °C increases the cracking index I_{cr} by approximately 1.6%. This indicates that the initial temperature of the concrete mix is a technological factor that directly and significantly affects the thermal cracking index, thus directly influencing thermal crack control measures. Therefore, a comprehensive thermal crack control plan must consider the initial temperature of the fresh concrete mix.

c. Effects of type of formwork

Formwork not only shapes the concrete but also influences its curing process and thermal management. The heat from the center of mass concrete is transferred to the environment through the

formwork system. As a result, the material of the formwork is an important factor affecting this heat transfer process. In modern concrete construction, various types of formwork made from different materials serve multiple functions including wood, metal, plastic, and combinations thereof [21]. Advances in concrete technology have introduced metal formwork, which is durable and can be used repeatedly throughout the construction process [19, 28]. To enhance its thermal insulation properties, various insulating materials are applied [29]. To assess the impact of formwork types on the thermal cracking index, numerical models will be analyzed with input materials as shown in Table 1, the analysis model as shown in Fig. 5, and changes in the formwork type used: (i) steel formwork, (ii) wood formwork, (iii) aluminum formwork, and (iv) plastic formwork, as indicated in Table 6.

The analysis results show that with the solution to control thermal cracking in large concrete blocks as mentioned above, the concrete block using formwork with a lower thermal conductivity tends to have a higher maximum temperature at the core, but the difference is not significant. For the solution using plastic formwork, $T_{\max}$ = 67.8 °C, while the solution using aluminum formwork has $T_{\max}$ = 66.8 °C, as illustrated in Fig. 7(a) and Table 6. Considering the thermal cracking index I_{cr}, it can be seen that I_{cr} increases when using formwork with lower thermal conductivity. At 120 hours after pouring, the concrete block using aluminum formwork has an I_{cr} = 0.70, while the samples of the concrete blocks using steel, wood, and plastic formwork have I_{cr} values of 0.72, 0.74, and 0.88, respectively, as shown in Fig. 7(b) and Table 6. Thus, with the given structure and materials, it can be observed that formwork materials with lower thermal conductivity tend to be more beneficial for thermal cracking control.

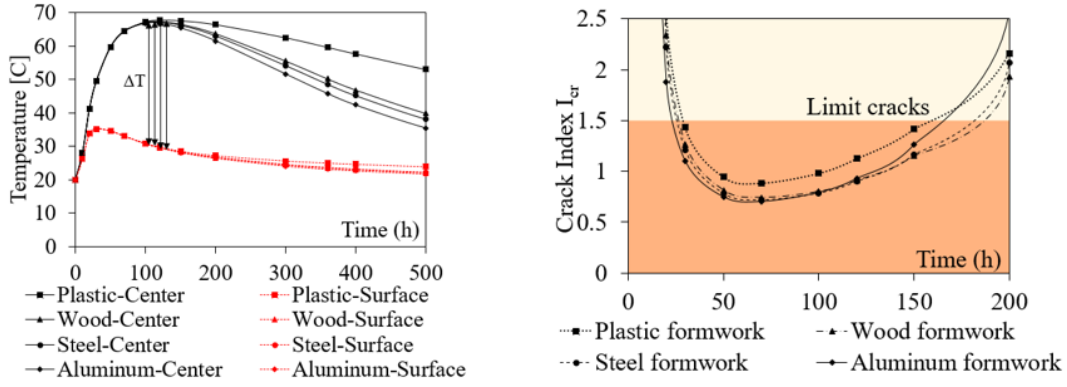

(a) The temperature gradient between the center and the surface

(b) Crack index

Figure 7. Effects of formwork on the temperature regime of mass concrete

Table 6. Effect of formwork type on the temperature regime in the mass concrete

No	Type of formwork	Thermal conductivity coefficient		Temperature regime			
		(W/m^2.°C)	kcal/(h.m^2.°C)	$T_{\max}$ (°C)	ΔT (°C)	I_{cr} (min)	Time (h)
1	Plastic formwork	0.5	0.43	67.8	38.1	0.88	120
2	Wood formwork	8.0	6.88	67.4	37.7	0.74	120
3	Steel formwork	14.0	12.04	67.2	37.6	0.72	120
4	Aluminum formwork	205.0	176.27	66.8	36.1	0.70	100
5	Ambient	12.0	10.32	-	-	-	-

d. Effects of the cement type

Different types of cement generate varying amounts of heat, therefore, they will directly affect the stress field and temperature development in the concrete mass [29]. Four types of cement commonly used according to the Japan Cement Association will be utilized to investigate the influence of cement type on the thermal regime in mass concrete: (i) normal Portland cement, (ii) moderate-heat Portland cement, (iii) high-early-strength Portland cement, and (iv) Portland blast-furnace slag cement. Note here that for each analysis model, the cement content and all boundary condition parameters are the same. The temperature development of the mass concrete is mainly governed by the heat source from the types of cement, as presented in Section 2.2. In this study, internal heat of hydration was estimated by an exponential function which is mainly based on adiabatic temperature rise and the coefficient of temperature rise. These values are defined based on default values suggested in Midas/Gen [27].

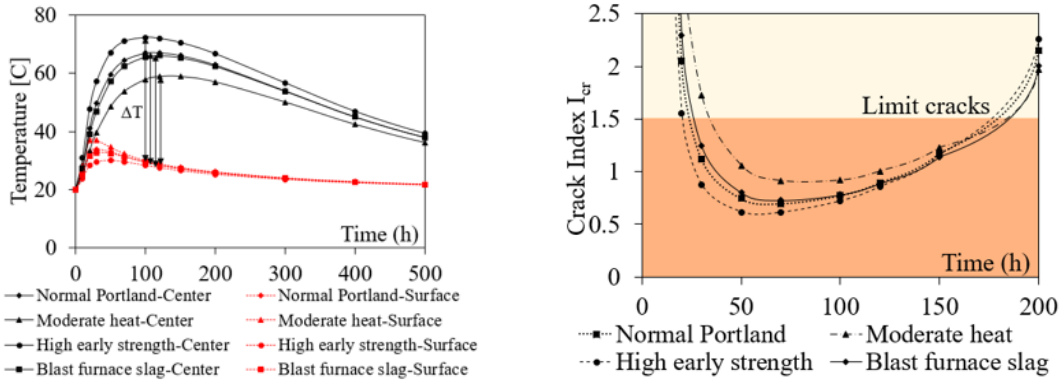

(a) The temperature gradient between the center and the surface

(b) Crack index

Figure 8. Effects of the cement type on the temperature regime of mass concrete

Table 7. The effect of type of cement on the temperature regime of mass concrete

No	Type of cement	Temperature regime of mass concrete			
		T_{max} (°C)	ΔT (°C)	I_{cr} (min)	Time (h)
1	Normal Portland	67.1	38.7	0.69	120
2	Moderate-heat Portland	58.9	31.4	0.91	150
3	High-early-strength Portlan	72.4	43.1	0.61	100
4	Portland blast-furnace slag	66.1	37.6	0.72	120

The temperature development curves at the center and surface of the concrete mass for different types of cement are illustrated in Fig. 8(a), while the crack index over time for the corresponding types of cement is compared in Fig. 8(b). Analysis results from the program indicate that the temperature gradient between the center and the surface ΔT is greatest when using high-early-strength Portland cement, with ΔT = 43.1 °C. This ΔT value is lower when using normal Portland cement, with ΔT = 38.7 °C; Portland blast-furnace slag cement, with ΔT = 37.6 °C; and lowest when using moderate-heat Portland cement, with ΔT = 31.4 °C. As shown in Fig. 8(b), the thermal crack index with the maximum tensile force turned out to be 0.91 when using moderate-heat Portland cement. The thermal crack index of the mass concrete with high-early-strength Portland cement was the lowest among

mass concretes mixed with four types of cement, with I_{cr} = 0.61. Meanwhile, the crack index of the mass concrete when using normal Portland cement is I_{cr} = 0.69, and the corresponding value when using Portland blast-furnace slag cement is I_{cr} = 0.72, as shown in Table 7. It can be seen that using moderate-heat Portland cement for mass concrete is considered to be safer against potential cracks than using other types of cement.

e. Effects of cement content

The effects of cement content on temperature development in mass concrete are significant. Higher cement content generally leads to a higher heat of hydration, which can result in increased internal temperatures. Strategies to mitigate these effects include using supplementary cementing materials like ground granulated blast-furnace slag or fly ash, which lower the overall heat generation [30]. In this study, binder content will be fixed to ensure that the designed strength of the mass concrete is not changed, but cement content will be varied by supplementing with fly ash. It should also be noted here that fly ash is considered not to generate heat during hydration and changes in cement content will lead to changes in the heat of hydration and thus changes in the stress and temperature fields in the mass concrete. Furthermore, the maximum fly ash content that can replace cement while still maintaining the designed strength of concrete varies, but it is commonly up to 30% of the cement content [31, 32]. In this study, four cases will be investigated with varying fly ash content: (i) 0%, meaning no fly ash replacement; (ii) 10%; (iii) 20%; and (iv) the maximum fly ash replacement of 30%. As with other examples, while the fly ash content is varied, all other parameters are fixed. Moderate-heat Portland cement, which is most effective in limiting the heat of hydration, will be used for all four survey scenarios.

The temperature development curves at the center and surface of the concrete mass with different cement contents are illustrated in Fig. 9(a), while the cracking index over time corresponding to different cement contents is compared in Fig. 9(b). Analysis results show that reducing the cement content or increasing the fly ash content in the mix increases the cracking index I_{cr}, indicating a reduced risk of thermal cracking in the mass concrete. At 70 hours after pouring, the concrete mass without fly ash has I_{cr} = 0.68, but when the fly ash content is increased to 10%, the cracking index rises to I_{cr} = 0.76, and when the fly ash content is 20%, the cracking index increases to I_{cr} = 0.86. When the concrete mass uses up to 30% fly ash, the cracking index rises to I_{cr} = 0.97, as shown in Table 8. A quantitative assessment shows that for each 1% increase in fly ash content, the cracking index I_{cr} also

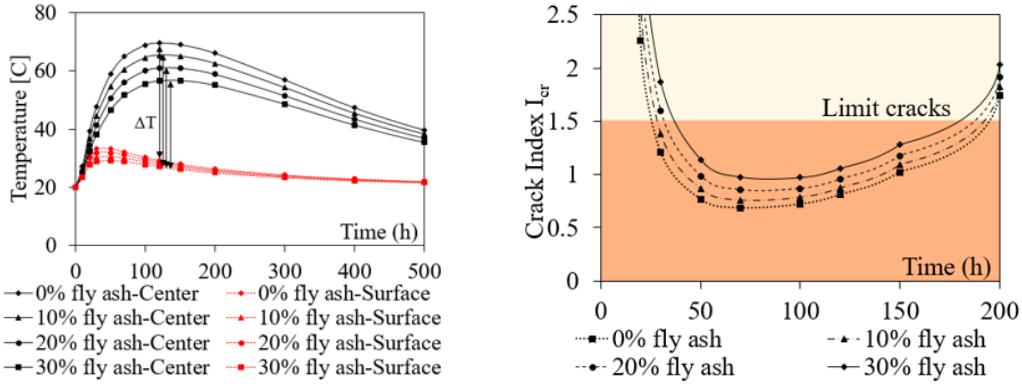

(a) The temperature gradient between the center and the surface

(b) Crack index

Figure 9. Effects of the cement content on the temperature regime of mass concrete

increases by 0.96%. From the temperature analysis perspective, the temperature gradient between the surface and the center ΔT is greatest when the cement content is not reduced, with ΔT = 40.4 °C. This ΔT value gradually decreases as the cement content is reduced, with ΔT = 36.7 °C if the cement content is decreased by 10%, ΔT = 33.2 °C if the cement content is reduced by 20%. When the cement content is reduced by 30%, the temperature difference between the center and the surface of the mass concrete is only ΔT = 29.5 °C, as shown in Table 8. Thus, it can be seen that adjusting the cement content, or effectively adding more fly ash, significantly affects the temperature development in mass concrete. Reduced cement content increases the cracking index, indicating a reduced risk of thermal cracking in the mass concrete.

Table 8. Effect of cement content on the temperature regime in the mass concrete

No	Content of cement (%)	Content of fly ash (%)	Temperature regime of mass concrete			
			$T_{\max}$ (°C)	ΔT(°C)	I_{cr} (min)	Time (h)
1	100	0	69.6	40.4	0.68	70
2	90	10	65.4	36.7	0.76	70
3	80	20	61.0	33.2	0.86	70
4	70	30	56.8	29.5	0.97	100

5. Conclusions

A comprehensive numerical study was conducted using the thermal analysis tool of Midas/Civil to evaluate the effects of construction technology factors on temperature development in mass concrete. Based on the research results, the following conclusions can be made:

- The concrete curing has significant effects on the thermal crack control in mass concrete. The higher the curing temperature, the higher the cracking index I_{cr}, which means that the foundation mass has a reduced risk of thermal cracks. For each 1 °C increase in the surface temperature of the mass concrete, the cracking index increases by approximately 1.5-2.0%. Therefore, an appropriate curing method should retain as much heat generated by the hydration process as possible.

- The lower the initial temperature of the concrete mix, the higher the cracking index I_{cr} of the concrete mass, meaning the risk of cracking is reduced. Correspondingly, for every 1 °C reduction in the initial temperature of the concrete mix, the cracking index I_{cr} increases by approximately 1.6%. This indicates that the initial temperature of the concrete mix is a technological factor that directly affects the thermal cracking index, and therefore, directly influences thermal crack control measures.

- Formwork materials with lower thermal conductivity tend to retain the heat generated by the hydration process better. Thus, using formwork with low thermal conductivity, such as wooden formwork, is more beneficial for thermal crack control.

- Using the moderate-heat Portland cement for mass concrete is likely safer against potential cracks than using other types of cement.

- Adjusting the cement content through adding more fly ash has significant effects on the temperature regime in mass concrete. Reduced cement content increases the cracking index, indicating a reduced risk of thermal cracking in the foundation mass. A quantitative assessment shows that for each 1.0% increase in fly ash content, the cracking index I_{cr} also increases by 0.96%.

References

[1] JCI (2008). *Guidelines for control of cracking of mass concrete*.

[2] Khalifah, H. A., Rahman, M. K., Al-Helal, Z., Al-Ghamdi, S. (2016). Stress generation in mass concrete blocks with fly ash and silica fume-an experimental and numerical study. In *Fourth International Conference on Sustainable Construction Materials and Technologies*, 7–11.

[3] Hai, T. H., Van Thuc, L. (2017). The effect of splitting concrete placement on controlling thermal cracking in mass concrete. *Journal of Science and Technology in Civil Engineering (JSTCE)-HUCE*, 11(6):22–28.

[4] Liu, W., Cao, W., Yan, H., Ye, T., Jia, W. (2016). Experimental and numerical studies of controlling thermal cracks in mass concrete foundation by circulating water. *Applied Sciences*, 6(4):110.

[5] Dabarera, A., Saengsoy, W., Kaewmanee, K., Mori, K., Tangtermsirikul, S. (2017). Models for predicting hydration degree and adiabatic temperature rise of mass concrete containing ground granulated blast furnace slag. *Engineering Journal*, 21(3):157–171.

[6] Choktaweekarn, P., Tangtermsirikul, S. (2010). Effect of aggregate type, casting, thickness and curing condition on restrained strain of mass concrete. *Songklanakarin Journal Of Science & Technology*, 32(4).

[7] Fairbairn, E. M. R., Azenha, M. (2019). *Thermal cracking of massive concrete structures*. State of Art Report of the RILEM TC.

[8] ACI Committee 207 (2005). *Guide to Mass Concrete (ACI 207.1R-05) (Reapproved 2012)*. American Concrete Institute, Farmington Hills, MI, 30.

[9] ACI Committee 207 (2005). *Cooling and Insulating Systems for Mass Concrete (ACI 207.4R-05) (Reapproved 2012)*. American Concrete Institute, Farmington Hills, MI, 15.

[10] ACI Committee 207 (2005). *Report on Roller-Compacted Mass Concrete (ACI 207.5R-11)*. American Concrete Institute, Farmington Hills, MI, 71.

[11] ACI Committee 207 (2005). *Report on Roller-Compacted Mass Concrete (ACI 207.5R-11)*. American Concrete Institute, Farmington Hills, MI, 71.

[12] ACI Committee 207 (2007). *Report on Thermal and Volume Change Effects on Cracking of Mass Concrete (ACI 207.2R-07)*. American Concrete Institute, Farmington Hills, MI, 28.

[13] Standard British (1986). *Structural use of concrete*. BS8110.

[14] SP 357.1325800.2017 (2016). *Concrete constractions of hydraulic structures. Rules of works and acceptance of works*. Ministry of construction and housing and communal services of the Russian Federation, 77.

[15] TCVN 9341:2012. *Mass concrete: Construction and acceptance*. Institute of Science and Technology and Construction, Ministry of Construction, Hanoi, 15.

[16] Taylor, H. F. W., Famy, C., Scrivener, K. L. (2001). Delayed ettringite formation. *Cement and Concrete Research*, 31(5):683–693.

[17] Ha, J.-H., Jung, Y. S., Cho, Y.-G. (2014). Thermal crack control in mass concrete structure using an automated curing system. *Automation in Construction*, 45:16–24.

[18] Lee, M. H., Khil, B. S., Yun, H. D. (2014). *Influence of cement type on heat of hydration and temperature rise of the mass concrete*. NISCAIR-CSIR, India.

[19] Onyekachukwu, E. P., Sharma, P., Singh, J. (2017). Review work on plastic formwork. *International Journal of Civil Engineering and Technology*, 8:1141–1146.

[20] Rahimi, A., Noorzaei, J. (2011). Thermal and structural analysis of roller compacted concrete (RCC) dams by finite element code. *Australian Journal of Basic and Applied Sciences*, 5(12):2761–2767.

[21] Zhang, X.-f., Li, S.-y., Li, Y.-l., Ge, Y., Li, H. (2011). Effect of superficial insulation on roller-compacted concrete dams in cold regions. *Advances in Engineering Software*, 42(11):939–943.

[22] Yun, T. S., Jeong, Y. J., Han, T.-S., Youm, K.-S. (2013). Evaluation of thermal conductivity for thermally insulated concretes. *Energy and Buildings*, 61:125–132.

[23] Bamforth, P., Chisholm, D., Gibbs, J., Harrison, T. (2008). *Properties of concrete for use in Eurocode 2*. Concrete Centre London.

[24] Abeka, H., Agyeman, S., Adom-Asamoah, M. (2017). Thermal effect of mass concrete structures in the tropics: Experimental, modelling and parametric studies. *Cogent Engineering*, 4(1):1278297.

[25] Institute Korea Concrete (2010). *Korean Concrete Standard Specification: Thermal Crack Control in Mass Concrete*. Kimoondang Publishing Company, Seoul, 166.

[26] Le, H.-H., Vu, C.-C., Ho, N.-K., Luu, V.-T. (2020). A method of controlling thermal crack for mass

concrete structures: modelling and experimental study. *IOP Conference Series: Materials Science and Engineering*, 869(7):072054.

[27] Midas IT (2004). *Midas/Civil User Manual, Ver. 6.3. 0 (Release no. 1)*. Midas IT Co, Ltd.

[28] Arslan, M., Şimşek, O., Subaşı, S. (2005). Effects of formwork surface materials on concrete lateral pressure. *Construction and Building Materials*, 19(4):319–325.

[29] Di Maio, A., Giaccio, G., Zerbino, R. (2002). Non-destructive tests for the evaluation of concrete exposed to high temperatures. *Cement, Concrete, and Aggregates*, 24(2):1–10.

[30] Woo, H.-M., Kim, C.-Y., Yeon, J. H. (2017). Heat of hydration and mechanical properties of mass concrete with high-volume GGBFS replacements. *Journal of Thermal Analysis and Calorimetry*, 132(1): 599–609.

[31] Association American Coal Ash (2003). *Fly ash facts for highway engineers*. US Department of Transportation, Federal Highway Administration.

[32] Mallisa, H., Turuallo, G. (2017). The maximum percentage of fly ash to replace part of original Portland cement (OPC) in producing high strength concrete. In *AIP Conference Proceedings*, 1903:030012.